Optimal Offloading Configuration of Spread-Moored FPSOs

Steven M. Wilkerson
Haynes Whaley Associates, Inc.,
2000 West Sam Houston Parkway South,
Suite 1800,
Houston, TX 77042

Satish Nagarajaiah
Department of Civil and Environmental Engineering,
Rice University,
P.O. Box 1892, MS318,
Houston, TX 77251-1892

As the oil offloading operations of floating production storage and offloading (FPSO) units become more routine, the desire grows to increase the availability for offloading and thus decrease production downtime. Experience with these operations is the main tool available to increase the efficiency of this aspect of deepwater production. However, it is clear that a formal optimization approach can help to fine tune design parameters so that not only is availability increased but the significance of each design parameter can be better understood. The key issue is to define the environmental conditions under which the vessels involved in offloading are able to maintain position. By this, we reduce the notion of availability to a set of operating criteria, which can or cannot be met for a particular set of environmental conditions. The actual operating criteria such as relative vessel heading depend on selection of design parameters, such as the direction and magnitude of external force applied by thrusters or tugs. In the earliest offloading operations, engineering judgment was used to determine the feasibility of offloading at a particular time. For example, if wind and current were not expected to exceed a 1 year return period, offloading may be considered safe. This approach can be both conservative and unconservative, depending on the nuances of the particular environmental conditions. This study will propose a formal approach to choosing the design parameters that optimize the availability of a FPSO for offloading. A simple analysis model will be employed so that optimization can be performed quickly using a robust second order method. The proposed analysis model will be compared to model test data to demonstrate its agreement with the more complex system. [DOI: 10.1115/1.2783886]

1 Introduction

In Fig. 1, we show the offloading of stored oil from a floating production storage and offloading (FPSO) unit to a shuttle tanker.[1] An early account of the design and field implementation of this procedure is given by Henriques [1]. According to that paper, the most important issue was to define the environmental conditions under which the vessels involved in offloading were able to maintain position. The set of such environmental conditions defines the availability, which is the fraction of time when an offloading procedure is viable. The FPSO in that account was offloaded on average every 10.5 days. The complete cycle of mobilizing the tanker, loading, demobilizing, and unloading lasted 8 days on average. With a single shuttle tanker to service it, the FPSO would essentially require offloading 75% of the time. Even in a very calm environment, it would be unusual to expect availability to be at that level. The efficiency is easily increased by using a fleet of shuttle tankers, but at some point downtime becomes inevitable because of weather conditions. This and other studies [2,3] demonstrate the need for optimizing offloading operations.

Offloading configurations may vary depending on the type and number of vessels involved [2]. Typical configurations consist of either the following:

- floating storage and offloading (FSO), Catenary anchor leg mooring (CALM) buoy, and tanker
- FPSO and tanker
- FSO, CALM buoy, tanker, and tug(s)
- FPSO, tanker, and tug(s)

Here, we concentrate on the final configuration, where the FPSO is spread moored, possibly with a compliant mooring system (shown schematically in Fig. 2). This sort of compliant mooring, called a differentiated compliant anchoring system (DICAS), is a hybrid of the regular spread-moored system and the turret moored system. The advantages are improved stability from the spread mooring, with the capability for limited weather vaning, as the FPSO is partially allowed to align with the direction of the prevailing environmental loads.

During offloading, the vessels are connected to each other by a polyester cable called a hawser. This limits relative movement of the vessels sufficiently so that a flexible pipe can be used to transfer the oil. Once they are connected, the vessels become a system whose equilibrium positions depend on one another and the magnitude and direction of environmental forces from wind, waves, and current. Design of an offloading procedure requires determination of a system that is safe as well as stable (that is, does not experience large motions). Safety requires sufficient clearance between the vessels and other necessary elements such as mooring lines and risers. Safety also requires structural integrity of the hawser line and the connections of the hawser to the vessel bulkheads. Morandini et al. [3] list the design variables that are pertinent to the offloading procedure as follows:

- relative vessel headings, to minimize the effects of yaw instability should fishtailing occur
- hawser tension, to avoid failure of the connections
- hawser azimuth, or direction to avoid collision during periods of transient weather and as the relative draft of the vessels increase and decrease
- distance between the vessels, to avoid collision

We add the tug or thruster force as a design variable. The net magnitude and direction of the stabilizing forces affect the other design variables and ultimately determine if maintaining equilibrium of the system is feasible with the use of tugs.

The issue of stability is addressed in advance, since uncontrolled motions would obviously preclude a safe offloading operation. Several studies [4,5] address this for turret moored or compliant moored systems. In general, instability is not considered to

[1]Internet photo from http://www.offshore-technology.com/projects/texaco/texaco7.html.

Contributed by the Ocean Offshore and Arctic Engineering Division of ASME for publication in the JOURNAL OF OFFSHORE MECHANICS AND ARCTIC ENGINEERING. Manuscript received December 6, 2005; final manuscript received January 19, 2007; published online March 24, 2009. Review conducted by Thomas E. Schellin.

Fig. 1 Offloading of a FPSO by shuttle tanker and tugs

be an issue for a conventional mooring system, since it can be designed to limit all in-plane motions of the FPSO including yaw so that large displacements are not possible. It has been shown [5] that for compliant moored (DICAS) systems, the shuttle tanker and tugs have a stabilizing effect on the overall system. Furthermore, use of proper physical limitations on the motions (such as limiting the absolute FPSO yaw) reduces the number of possible unstable equilibrium positions of the system. In this paper, we assume that the designated system is stable provided the motions have a reasonable level of constraint.

Proper analysis of the offloading procedure requires nonlinear dynamic analysis to determine mean equilibrium positions of the vessels and thus quantify the design variables. The most significant simplification taken here is the use of static, linear analysis to approximate the mean behavior of the system. This is necessary once optimization of the process is undertaken, due to the need for repeated analysis of the system as the optimization procedure converges to a solution. Use of expensive codes in optimization for "black box" analysis if warranted may be achieved with limited success (see, for example, Booker et al. [6]). Here, this would entail a nonlinear time history analysis including the effects of body interaction on the wave forces, full coupling of dynamic degrees of freedom, and nonlinear mooring and hawser line stiffness. However, the other limiting factors described in the paper by Booker et al., such as lack of derivatives or lack of a solution at infeasible points, do not exist in this case. Instead, a "simplified physics model" is used. In this approach, the system is described by simplified laws that are based on the actual physics of the problem, but are known to be inexact, or unsuitable outside of a particular range of variables. Thus, the linear, static analysis is adopted with the following limitations:

- The values of the variables predicted are consistent with the mean equilibrium positions of the vessels and should be adjusted to consider higher, but short duration episodic values. In particular, the design of the hawser should be amplified by an impact factor of at least 1.5 [1].
- Equivalent linear mooring line stiffness should be calculated for the expected mean position of the FPSO (see, for example, Ref. [7]). The absolute motions of the FPSO should be limited to reflect the applicable range of motion for this approximation.
- The hawser should have sufficient pretension so that it behaves as a linear spring.
- Motions out of the horizontal plane (heave, pitch, and roll) are negligible.
- The coupling of horizontal (in-plane) degrees of freedom is negligible, with the exception of the linearized mooring stiffness, which may be fully coupled.
- Sheltering or screening effects from multiple bodies on the wind, wave, and current forces are neglected.

The use of linear mooring and hawser stiffness is a common simplification even when more sophisticated analysis is used (e.g., see Refs. [8,9]). This simplification, in particular, is necessary whenever frequency domain methods are used. Here, the requirement for linear analysis is for speed of evaluating the equilibrium equations. Neglecting heave, pitch, and roll is acceptable for the configuration considered because of the stiffness of the mooring system, while neglecting the coupling of the in-plane degrees of freedom is commonly done (e.g., see Ref. [4]). The neglect of sheltering effects is largely a practical matter. The sheltering effect from wind and current requires detailed information and furthermore depends on the relative positions of the vessels. This level of detail is not generally available and so is not used. Use of a blanket reduction may be warranted (e.g., see Ref. [4]), but most often the effect is neglected (as in Refs. [2,3,5]). The analogous effect on wave forces is more commonly included through use of wave diffraction analysis but is sometimes neglected (e.g., see Ref. [8]).

Environmental loads are approximated by various conventional means. Details of the calculation of wind, current, swell, and local wave forces are given in Appendix A. The wind and current forces are based on the empirical data provided by the Oil Companies International Marine Forum (OCIMF) [10] for very large crude carriers (VLCCs) and are parametrized by their velocity. Current forces on risers are neglected for simplicity. Wave forces[2] are evaluated using an assumed distribution and parametrized by their significant wave height H_s and peak period T_p. The Gaussian spectrum is assumed for swells and is parametrized by a coefficient of variation σ. The Joint North Sea Wave Analysis Project (JONSWAP) spectrum is assumed for local waves and is parametrized by a coefficient of variation σ and a peak enhancement factor γ. Return periods are not strictly indicated but some guidelines are reviewed here. The use of a 10 year return period (as in Ref. [2]) is probably excessive, since offloading would not be feasible under these conditions. A 1 year return period is commonly accepted for design of offloading procedures (e.g., see Refs. [1,11]). Ideally, when annual site specific data are available, it can be used so that return periods need not be guessed. Additionally, a more clear picture of the duration of severe environmental conditions is gathered from the use of such data. All environmental loads depend on the loading condition of the FPSO and tanker. As this can vary between ballast and fully loaded condi-

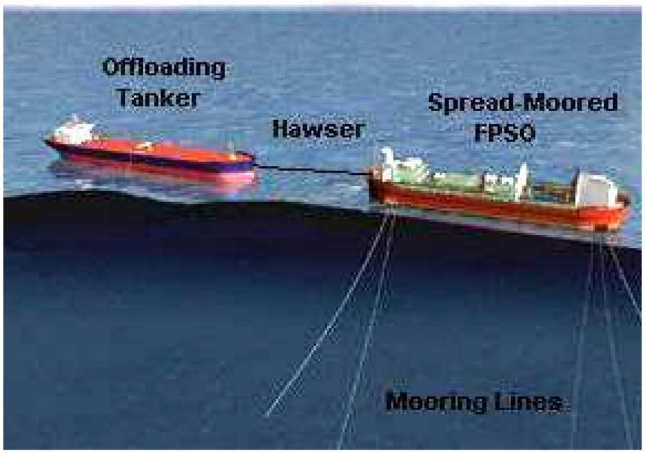

Fig. 2 Schematic diagram of the offloading procedure

[2]Swells and local waves are considered independently.

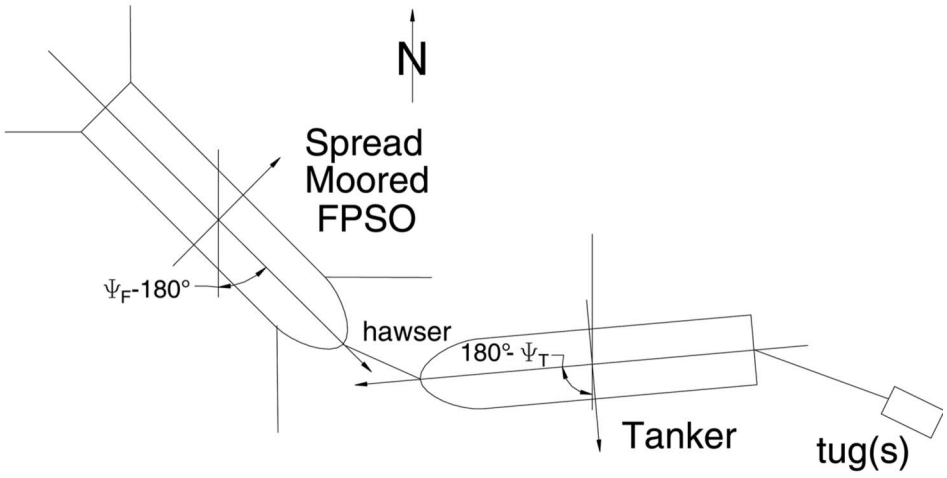

Fig. 3 Plan view of FPSO and tanker in bow-to-bow tandem offloading

tions, rational combinations of these should be considered (e.g., see Ref. [2]) for each set of environmental loads.

2 Optimal Offloading Availability Problem

The vessel configuration for bow-to-bow tandem offloading is shown in plan in Fig. 3: Compass north is the base line for global vessel headings. In the previous section, design variables for the optimal offloading problem were described. These consisted of vessel position information and tug and hawser force information. Again, all motion is restricted to the horizontal plane so that surge, sway, and yaw describe the full state of each vessel. A further simplification is made by assuming the relative drift between the FPSO and tanker is negligible to eliminate two of these variables. In practice, the hawser is considered inextensible and functions as a rigid link between the vessels. Similarly, the tug lines are considered inextensible, although tug motions are of no interest other than to define the direction of the net tug force. Accounting for all of the variables, we have the following:

1. x-direction drift Δx
2. y-direction drift Δy
3. FPSO heading Ψ_F
4. tanker heading Ψ_T
5. tug force F_t
6. tug angle ψ_t
7. hawser force F_h, and
8. hawser angle ψ_h

The subscripts refer to each component of the system such as F for FPSO, T for tanker, t for tug, etc. The drifts Δx and Δy refer to the total system drift, and are therefore not subscripted.

Six of the variables define the state of the system. Six equations of equilibrium, arrived at by summing forces and moments at the center of gravity of each vessel, are necessary and sufficient to determine the state variables. The remaining variables, the hawser and tug forces, are free variables, which may be chosen to optimize a certain objective. Here, we choose to minimize the magnitude of the tug force. This is consistent with the objective of increasing availability. When the tug force required to maintain equilibrium is below a certain threshold level (defined by economic or practical limitations), the offloading procedure is viable.

For convenience, a change of variables is made so that the FPSO yaw $\Delta\Psi_F$ is used as a primary variable in place of the heading Ψ_F. By doing this, the surge, sway, and yaw of the FPSO become primary variables, which are directly related to the mooring reactions. The FPSO heading is then taken as the mean heading plus the yaw ($\Psi_F = \Psi_{F_0} + \Delta\Psi_F$). Another change is made by using components of the tug force (F_{xt} and F_{yt}) and hawser force (F_{xh} and F_{yh}) instead of their magnitude and direction. This is done to decrease the nonlinearity of the equilibrium equations. Incorporating operational limitations discussed earlier, the offloading optimization problem is then formally stated as

$$\min_x F_t(x) \tag{1}$$

subject to

$$c(x) = 0$$

$$\Delta(x) \le r_{\max}$$

$$|\Delta\Psi_F| \le \psi_{F_{\max}}$$

$$|\psi_T(x)| \le \psi_{T_{\max}}$$

$$F_{xt} < 0$$

$$F_{xh} > 0$$

$$F_{h_{\min}} \le F_h(x) \le F_{h_{\max}}$$

$$|\psi_t(x) - 180| \le \psi_{t_{\max}}$$

$$|\psi_{hT}(x)| \le \psi_{h_{\max}}$$

$$|\psi_{hF}(x)| \le \psi_{h_{\max}}$$

where $x = [\Delta x\ \Delta y\ \Delta\Psi_F\ \Psi_T\ F_{xt}\ F_{yt}\ F_{xh}\ F_{yh}]^T$, $F_t(x) = \sqrt{F_{xt}^2 + F_{yt}^2}$ is the objective function, $c(x)$ are the equilibrium constraints, $\Delta(x) = \sqrt{\Delta x^2 + \Delta y^2}$, $F_h(x) = \sqrt{F_{xh}^2 + F_{yh}^2}$, $\psi_T(x) = \Psi_T - \Psi_F(x) - 180$, $\psi_t(x) = \tan^{-1}(F_{yt}/F_{xt})$, $\psi_{hT}(x) = \tan^{-1}(F_{yh}/F_{xh})$ (with respect to the tanker), $\psi_{hF}(x) = \Psi_T - 180 - \Psi_F(x) + \psi_{hT}(x)$ (with respect to the FPSO), $r_{\max}$ is a bound on FPSO drift (the watch circle radius), $\psi_{F_{\max}} < 90$ is a bound on FPSO yaw, $\psi_{T_{\max}} < 90$ is a bound on tanker and FPSO relative yaw, $F_{h_{\min}}$ is the hawser pretension force, $F_{h_{\min}}$ is an upper bound on the hawser force, $\psi_{t_{\max}} < 90$ is a bound on the tug angle, and $\psi_{h_{\max}} < 90$ is a bound on the hawser angle.

The equilibrium constraints will be described in detail in Sec. 2.2.1. Limits are imposed on the FPSO drift and yaw as operational restrictions as well as limiting the range of motion applicable to the linearized stiffness approximation. Operational limits are imposed on the relative heading between the tanker and FPSO,

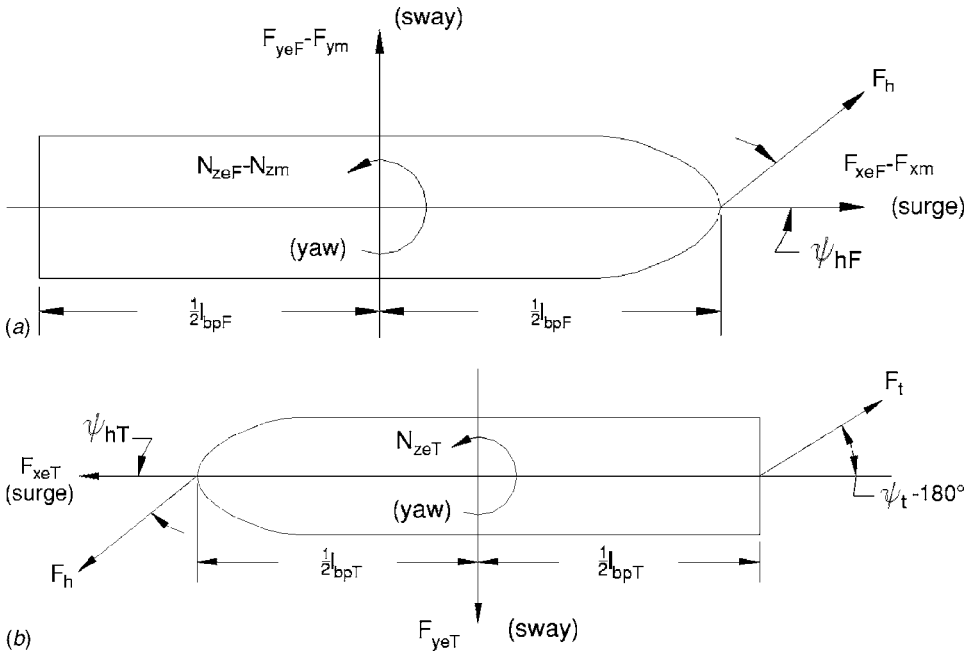

Fig. 4 Free body equilibrium of tanker and FPSO

and angle of the hawser and tug lines. Lower and upper bound limits are imposed on the hawser force. The x components of the tug and hawser forces are limited for two reasons. Each must be bounded away from zero to prevent division by zero in the expression for tug and hawser angles. The sign of each is limited (along with the limit on tug and hawser angles) to guarantee that the tug and hawser lines are always in tension.

The possibility of multiple equilibrium positions exists because the state equations are nonlinear in x (see Sec. 2.2.1). Use of operational limits on the variables reduces the number of potential equilibrium positions. It also eliminates a number of unstable positions of the DICAS (see Ref. [5]). Problem 1 is nonconvex and has multiple local solutions for each set of vessel and environmental parameters. Various loading conditions (FPSO and tanker draft) will also give rise to different local minima because the environmental loads are a function of the draft. It is important to obtain a reasonable guess to the solution because that will affect the local optima obtained as a solution. Use of various starting solutions may be useful to study the quality and number of local optima. Finally, the inequality constraints in Problem 1 may be recast to an equivalent form so that the equations are less nonlinear (e.g., see Ref. [12], Chap. 7). This step may make the optimization more efficient since the constraints are linearized during the solution iterations.

Solution of Problem 1 can be done using software for constrained optimization (e.g., see Ref. [12]). An efficient second order method such as a sequential quadratic programming (SQP) or an interior point method is most suitable, since derivatives of the objective and constraints are readily available. Partial derivatives of various functions in the formulation are given in Appendix A.2 for reference. In general, optimization algorithms require first derivatives (gradients) of the objective function and constraint equations. Second derivatives of the objective function are not necessarily required, since secant approximations can be easily obtained.

2.1 Equilibrium and Feasibility. We study local equilibrium by considering free bodies of the FPSO and tanker. Forces on the FPSO include the environmental loads, hawser force, and the mooring reactions (see Fig. 4(a)). Equilibrium of the FPSO is defined by

$$\begin{bmatrix} F_{xeF}(x) + F_h(x)\cos(\psi_{hF}(x)) \\ F_{yeF}(x) + F_h(x)\sin(\psi_{hF}(x)) \\ N_{zeF}(x) + \frac{1}{2}l_{pbF}F_h(x)\sin(\psi_{hF}(x)) \end{bmatrix} = \begin{bmatrix} F_{xm}(x) \\ F_{ym}(x) \\ N_{zm}(x) \end{bmatrix}$$

where l_{bpF} is the FPSO length.

F_{xeF}, F_{yeF}, and N_{zeF} are the net FPSO environmental loads,

$$\begin{bmatrix} F_{xm}(x) \\ F_{ym}(x) \\ N_{zm}(x) \end{bmatrix} = \mathbf{K}_F \begin{bmatrix} \Delta x \\ \Delta y \\ \Delta\Psi_F \end{bmatrix}$$

$\mathbf{K}_F$ is the 3×3 linearized mooring stiffness matrix.

Forces on the tanker include the environmental loads, hawser force, and tug force (see Fig. 4(b)). Equilibrium of the tanker is defined by

$$\begin{bmatrix} F_{xeT}(x) + F_{xT} + F_{xh} \\ F_{yeT}(x) + F_{yT} + F_{yh} \\ N_{zeT}(x) - \frac{1}{2}l_{bpT}F_{yT} + \frac{1}{2}l_{bpT}F_{yh} \end{bmatrix} = \begin{bmatrix} 0 \\ 0 \\ 0 \end{bmatrix}$$

where l_{bpT} is the tanker length. F_{xeT}, F_{yeT}, and N_{zeT} are the net tanker environmental loads.

After grouping the FPSO and tanker equilibrium equations into six system equations and subtracting the right hand sides, the resulting state equations are obtained:

$$c(x) = \begin{bmatrix} F_{xeT}(x) + F_{xt} + F_{xh} \\ F_{yeT}(x) + F_{yt} + F_{yh} \\ N_{zeT}(x) - \frac{1}{2}l_{bpT}F_{yt} + \frac{1}{2}l_{bpT}F_{yh} \\ F_{xeF}(x) + F_h(x)\cos(\psi_{hF}(x)) - F_{xm}(x) \\ F_{yeF}(x) + F_h(x)\sin(\psi_{hF}(x)) - F_{ym}(x) \\ N_{zeF}(x) + \frac{1}{2}l_{bpF}F_h(x)\sin(\psi_{hF}(x)) - N_{zm}(x) \end{bmatrix} \quad (2)$$

2.2 Environmental Loads. The environmental loads due to wind, current, and waves (swell and local waves) are estimated using various conventional means. The wind and current loads are calculated using OCIMF [10] coefficients derived for VLCCs. The wave forces are calculated using a similar scheme with precalculated force coefficients. These were derived in advance using a finite panel method and wave diffraction analysis (e.g., see Ref. [9]) for vessels of comparable size and hydrodynamic properties. Appendix A.1 describes the procedure in more detail.

The net loads are the sum of contributions from wind, current, swell, and local waves. Each depends on the relative heading between the vessel and the predominant direction of the environmental load. Since the environmental load parameters (speed, significant wave height, heading, etc.) are fixed in the optimization problem, the net environmental loads depend only on the relative heading, or more generally the FPSO or tanker heading. In each case, the forces have been discretized at relative headings for a 10 deg interval, 0,10,20,…,360. Since the environmental loads are periodic (with period 2π), $F(0)=F(360)$ for each. For headings in between the discrete values, the loads are approximated using linear or cubic spline interpolation. It has been shown [12] that the use of cubic splines results in a smoother problem requiring fewer iterations of the optimization algorithm.

3 Examples and Model Validation

Model test data of a compliant moored FPSO with a shuttle tanker [11] are used to verify the calculation of environmental loads and mean equilibrium positions using the proposed static, linear model. Model test verification is an important step in validating the optimization results; however, this is not a rigorous approach. We seek only to show that the model reproduces trends in the experimental data, without excessive error. In order to prove convergence to the "true optimal solution," it is necessary to use a model management framework and validate the simplified model with a high-fidelity physics model (see Ref. [6] and also Ref. [13]). Again, it is desirable to avoid expensive simulations, so that a large number of problems can be solved with a reasonable degree of accuracy.

The benchmark study was conducted on 1:104 scale models of the vessels in a 30×20 m^2 wave tank. Swells were generated with a hydraulically driven flap wavemaker system. Current was generated by an underwater array of nozzles. Wind and local waves were generated by three fans mounted along the edge of the basin. All environmental loads (see also Appendix A.1) applied to the FPSO and tanker assume a 1 year return period:

- wind, $V_w=13$ m/s
- current, $V_c=0.8$ m/s
- swell, $H_{ss}=3.14$ m, $T_{ps}=15.7$ s
- local waves, $H_{sa}=1.4$ m, $T_{pa}=5.0$ s

Both the FPSO and tanker were based on a (full size) 300,000 DWT vessel with length of 332 m, breadth of 52.6 m, depth of[3] of 28.0 m, draft (ballast) of 9.36 m, and draft (full) of 20.8 m. The superstructure wind areas were assumed equal to zero. The configuration in the testing was bow-to-stern tandem offloading so that the local axis system of the tanker is offset by 180 deg.

The specifics of the mooring line stiffness are not given in the paper, but a compliant system was used, which allowed yaw of the FPSO up to 55 deg. The analysis assumes an uncoupled mooring stiffness with

[3]The depth is not reported by Codiglia et al. [11], but the value given here is a typical value for VLCCs and is consistent with the results.

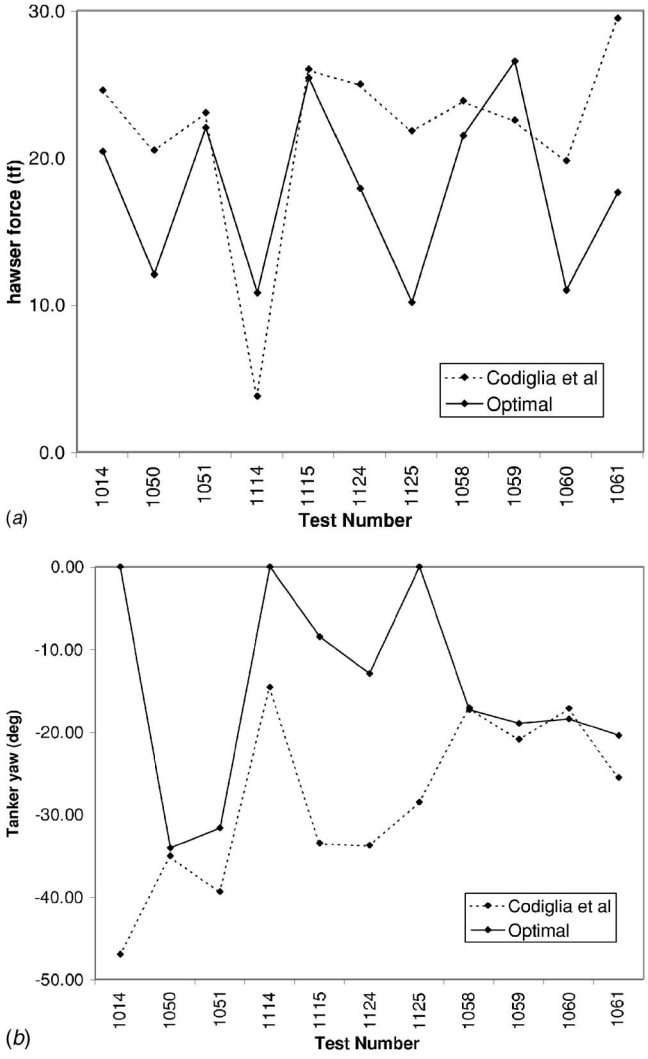

Fig. 5 Comparison of model tests [11] with optimal solution

$$\mathbf{K}_F=\begin{bmatrix} 10\ \text{tf/m} & 0 & 0 \\ 0 & 10\ \text{tf/m} & 0 \\ 0 & 0 & 100\ \text{tf m/deg} \end{bmatrix}$$

which produces stiff lateral springs, and a relatively flexible rotational spring. Operational limits imposed were

$$r_{\max}=10{,}000\ \text{m}$$

$$\psi_{F\,\max}=55\ \text{deg},\quad \psi_{T\,\max}=45\ \text{deg}$$

$$F_{h\,\min}=1\ \text{tf},\quad F_{h\,\max}=100\ \text{tf}$$

$$\psi_{t\,\max}=85\ \text{deg},\quad \psi_{h\,\max}=85\ \text{deg}$$

Because of insufficient information to properly define the lateral springs, a large watch circle radius was taken (10,000 m) to avoid invalid solutions with active surge and sway constraints.

This analysis attempts to show that the tanker equilibrium position and hawser force are consistent with the model test results. The experimental and optimal results are compared for the hawser force (Fig. 5(*a*)) and the tanker yaw (Fig. 5(*b*)). Several redundant cases were omitted from the figures for simplicity. Additionally, all of the beam-on sea cases were omitted because a stern line was used to control the motions of the tanker, and no information was made available about the nature of the force in the line. FPSO motion data were not compared as mean values were not reported

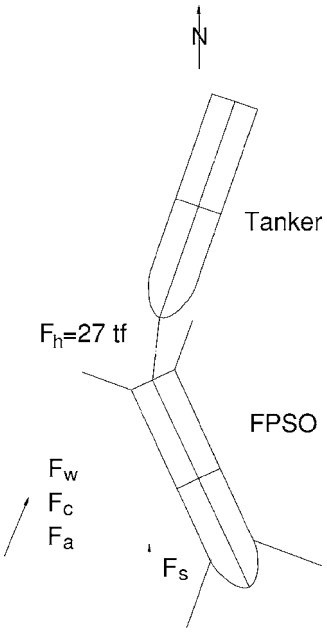

Fig. 6 Optimal equilibrium configuration of Test No. 1059 Codiglia et al. [11]

in the study. Also, since the mooring line stiffness was not reported, the mooring line forces and lateral displacements of the tanker and FPSO were not compared.

The agreement is good for hawser force with the trend being reproduced well. With the exception of Test No. 1014, the trend of the tanker yaw is in good agreement as well. This particular case was reportedly head-on seas, so that the optimal 0 deg yaw is consistent with the environmental parameters. Overall, only a qualitative comparison of the results is possible, which was considered sufficient for the purpose of validating the simplified physics model.

A particular case from the testing is now reproduced in detail here for clarity. Test No. 1059 was conducted with a fully loaded FPSO and ballasted tanker. The test gives reasonably good agreement between the static, linear model and the experimental results. The mean experimental hawser force of 23 tf is about 18% lower than the optimal value of 27 tf. The mean experimental tanker yaw of −21 deg is about 9% larger than the optimal value of −19 deg. The optimal equilibrium position of the tanker and FPSO is shown in Fig. 6. The optimal solution (x^*) is given in Table 1. No tug force is shown in either the figure or table, since the optimal solution was a zero tug force. The swell angle of attack was due north, while the wind, current, and local waves were at a heading of −22.5 deg. A summary of the optimal environmental loads for the tanker and FPSO is given in Table 2.

Without the presence of a tug, the tanker must align with the prevailing environmental loads. Figure 6 shows that the heading of the tanker is nearly coincident with the wind, current, and local waves, but biased slightly toward the direction of the swells. The hawser is the only force on the tanker that offsets the environmental loads. The components F_{xh} and F_{yh} are equal to the net surge and sway force produced by the environmental loads. The hawser is optimally aligned so that its beam-on force component across the tanker bow produces a righting yaw moment just equal to the net moment from the environmental loads.

The FPSO, on the other hand, does not align directly with the environmental loads since the mooring lines are available to provide stability. Note that the yaw angle of the FPSO is relatively large so that some weathervaning does take place. The mooring reactions in the x and y directions are equal to the net force on the FPSO produced by environmental loads and the hawser. The yaw moment from environmental loads is offset by a combination of the hawser moment and the yawing stiffness from the mooring lines. The large righting moment produced by the hawser explains how the optimal heading of the FPSO came about: Although it has not aligned with the prevailing environmental loads, the equilibrium position is such that the combination of both hawser force and mooring lines provides significant stability to the FPSO.

The equilibrium of the tanker and FPSO are determined by Eq. (2). The other conditions for an optimal solution are seen by reviewing Problem 1. From the solution, it is seen that the only active inequality constraint is $F_{xt} < 0$. In practice, a constraint tolerance of -10^{-4} is used so that even though the tug force is essentially zero, the x component is numerically less than zero. The only other condition for an optimal solution is that the objective function or F_t is minimized. Although it is possible to prove that the solution x^* given above is optimal, this is not necessary, since clearly the lower bound on the tug force is zero.

Table 1 Optimal solution of Test No. 1059 of Codiglia et al. [11]

Variable	Optimal value
Δx	−3.1 m
Δy	14 m
$\Delta\Psi_F$	25 deg
Ψ_T	160 deg
F_{xt}	0 tf
F_{yt}	0 tf
F_{xh}	26 tf
F_{yh}	6.3 tf

Table 2 Optimal environmental loads on tanker and FPSO for Test No. 1059 of Codiglia et al. [11]

	Tanker			FPSO		
Load	F_x (tf)	F_y (tf)	N_z (tf m)	F_x (tf)	F_y (tf)	N_z (tf m)
Wind	−9.0	2.7	150	−2.1	13	−540
Current	−5.2	2.3	110	2.1	88	3800
Swell	−8.7	−11	−1300	−4.4	6.7	790
Local waves	−2.4	0.58	77	−3.2	18	630
Tug	0	0	0	—	—	—
Hawser	26	6.3	1000	−23	13	−2200
Mooring	—	—	—	31	−140	2500

4 Conclusions

A formal statement of the problem for optimization of FPSO availability has been given. It has been proposed that by minimizing the tug (or thruster) force applied to stabilize the tanker during offloading, the feasibility of offloading can be determined as a practical matter when the tug force is within economical limits. The primary factor affecting availability is the prevailing environmental loads, but by varying design parameters such as the FPSO heading, the effect of external loads may be reduced. Additionally, operational limitations on the offloading must be imposed, further affecting availability. These are quantified by using constraints, or bounds on certain parameters such as the relative heading between the FPSO and tanker.

By stating the question of availability as a constrained optimization problem, the equilibrium of the system (FPSO and tanker) is connected directly to the problem via a set of equality constraints. The dependency of environmental loads on the vessel heading makes essential the integrated method of solving for equilibriums while minimizing tug forces. It was demonstrated in Sec. 3 (Test No. 1059) that a particular set of vessel headings is best suited to a given set of environmental loads, and by choosing these headings properly, a very small (in that case, zero) tug force was required to stabilize the tanker.

If annual weather data are available for a particular site, the study of offloading availability may be conducted by repeatedly solving Problem 1 for each anticipated set of environmental loads and a rational combination of vessel loading conditions. An upper bound on the expected availability can be easily determined through such a study, helping to forecast expected production downtime. In lieu of using site specific data, wind, current, and wave forces for a 1 year recurrence interval can be used in simulations where the headings of the environmental loads are varied using a Monte Carlo simulation. This type of approach may be used to estimate mean availability as well as upper and lower bounds with certain confidence.

Acknowledgment

The authors would like to thank the Houston Office of Shell International Exploration and Production for the financial support of this research.

Appendix

A.1 Environmental Loads

This section details the equations used to calculate environmental loads based on vessel parameters and basic environmental data.

The vessel dimensions and exposed superstructure areas are generically referred to by the following: l_{bp} is the length between vessel perpendiculars (m), b is the vessel beam (m), d is the vessel depth (m), f is the vessel simulation freeboard (m), A_{st} is the head on projected area of the superstructure (m^2), and A_{sl} is the beam on projected area of the superstructure (m^2).

Physical constants used are the following: $g=9.81\ m/s^2$ is the acceleration of gravity, $\gamma_a=1.25\times10^{-3}\ tf/m^3$ is the specific weight of air, $\gamma_w=1.03\ tf/m^3$ is the specific weight of seawater, $\rho_a=\gamma_a/g$ is the density of air, and $\rho_w=\gamma_w/g$ is the density of seawater.

The wind loads (in tf) acting on a vessel at heading Ψ are the following:

$$F_{xw}(\theta_w;V_w)=\frac{1}{2}\rho_a V_w^2 C_{xw}(\theta_w)(bf+A_{st})$$

$$F_{yw}(\theta_w;V_w)=\frac{1}{2}\rho_a V_w^2 C_{yw}(\theta_w)(l_{bp}f+A_{sl})$$

$$N_{zw}(\theta_w;V_w)=\frac{1}{2}\rho_a V_w^2 C_{zw}(\theta_w)l_{bp}(l_{bp}f+A_{sl})$$

where $\theta_w=\Theta_w-\Psi$ is the relative wind heading, Θ_w is the absolute wind heading, V_w is the wind speed (m/s), and C_{xw}, C_{yw}, and C_{zw} are OCIMF [10] wind force coefficients.

The current loads (in tf) acting on a vessel at heading Ψ are the following:

$$F_{xc}(\theta_c;V_c)=\frac{1}{2}\rho_w V_c^2 C_{xc}(\theta_c)b(d-f)$$

$$F_{yc}(\theta_c;V_c)=\frac{1}{2}\rho_w V_c^2 C_{yc}(\theta_c)l_{bp}(d-f)$$

$$N_{zc}(\theta_c;V_c)=\frac{1}{2}\rho_w V_c^2 C_{zc}(\theta_c)l_{bp}^2(d-f)$$

where $\theta_c=\Theta_c-\Psi$ is the relative current heading, Θ_c is the absolute current heading, V_w is the current speed (m/s), and C_{xc}, C_{yc}, and C_{zc} are OCIMF [10] current force coefficients.

For swell and local waves, drift force coefficients C_{xd}, C_{yd}, and C_{zd} are estimated in advance by simulation using wave diffraction analysis in WAMIT® for reference periods, $0.5\leqslant T\leqslant 20$ s and relative headings, $0\ deg\leqslant\theta\leqslant 360\ deg$.

For swell, a Gaussian spectrum is assumed. For a reference period, T:

$$S_s(T;H_{ss},T_{ps},\sigma)=\left(\frac{H_{ss}}{4}\right)^2\frac{T_{ps}}{\sigma\sqrt{2\pi}}\exp\left[-\frac{(T_{ps}/T-1)^2}{2\sigma^2}\right]$$

where H_{ss} is the significant wave height of swells, T_{ps} is the peak period of swells, and σ is the coefficient of variation, taken as 0.1.

The swell loads (in tf) acting on a vessel at heading Ψ are the following:

$$F_{xs}(\theta_s)=\gamma_w b\int_0^\infty\frac{1}{T^2}S_s(T;H_{ss},T_{ps},\sigma)C_{xd}(T,\theta_s)dT$$

$$F_{ys}(\theta_s)=\gamma_w l_{bp}\int_0^\infty\frac{1}{T^2}S_s(T;H_{ss},T_{ps})C_{yd}(T,\theta_s)dT$$

$$N_{zs}(\theta_s)=\gamma_w l_{bp}^2\int_0^\infty\frac{1}{T^2}S_s(T;H_{ss},T_{ps})C_{zd}(T,\theta_s)dT$$

where $\theta_s=\Theta_s-\Psi$ is the relative swell heading and Θ_s is the absolute swell heading.

For local waves, a JONSWAP spectrum is assumed. For a reference period, T:

$$S_a=(T;H_{sa},T_{pa},\alpha,\sigma,\gamma)=5\alpha\left(\frac{H_{sa}}{4}\right)^2 T\left(\frac{T}{T_{pa}}\right)^4\exp\left[-\frac{5}{4}\left(\frac{T}{T_{pa}}\right)^4\right]\gamma^r$$

where H_{sa} is the significant wave height of local wave, T_{pa} is the peak period of local wave, and

$$r=\exp\left[-\frac{(T_{pa}/T-1)^2}{2\sigma^2}\right]$$

The coefficient of variation is taken as

$$\sigma=\begin{cases}0.07 & T_{pa}\leqslant T\\ 0.09 & T_{pa}>T\end{cases}$$

γ is a peak enhancement factor, taken as 3.3, and α is a normalization factor, taken as 0.656.

The local wave loads (in tf) acting on a vessel at heading Ψ are the following:

$$F_{xa}(\theta_a) = \gamma_w b \int_0^\infty \frac{1}{T^2} S_a(T;H_{sa},T_{pa}) C_{xd}(T,\theta_a) dT$$

$$F_{ya}(\theta_a) = \gamma_w l_{bp} \int_0^\infty \frac{1}{T^2} S_a(T;H_{sa},T_{pa}) C_{yd}(T,\theta_a) dT$$

$$N_{za}(\theta_a) = \gamma_w l_{bp}^2 \int_0^\infty \frac{1}{T^2} S_a(T;H_{sa},T_{pa}) C_{zd}(T,\theta_a) dT$$

where $\theta_a = \Theta_a - \Psi$ is the relative local wave heading and Θ_a is the absolute local wave heading.

Note that in all cases, force coefficients C_{xx}, C_{yx}, and $C_z x$ are adjusted for the simulation freeboard.

A.2 Derivatives of the Objective and Constraint Functions

This section gives the gradients of the equations in the offloading optimization problem. The gradient of a multivariate function f: $IR^n \rightarrow IR$ is given by

$$\nabla f = \begin{bmatrix} \partial f/\partial x_1 \\ \partial f/\partial x_2 \\ \vdots \\ \partial f/\partial x_i \\ \vdots \\ \partial f/\partial x_n \end{bmatrix}$$

where $\partial f/\partial x_i$ is the partial derivatives of f with respect to x_i.

Partial derivatives, when nonzero, are given below for all functions in the formulation depending on x (see Problem 1 and Eq. (2)).

A.2.1 Objective Function

$$F_t(x) = \sqrt{F_{xt}^2 + F_{yt}^2}$$

$$\frac{\partial F_t}{\partial F_{xt}} = \frac{F_{xt}}{F_t} \quad \frac{\partial F_t}{\partial F_{yt}} = \frac{F_{yt}}{F_t}$$

A.2.2 Miscellaneous Constraint Functions

$$\Delta(x) = \sqrt{\Delta x^2 + \Delta y^2}$$

$$\frac{\partial \Delta}{\partial \Delta x} = \frac{\Delta x}{\Delta} \quad \frac{\partial \Delta}{\partial \Delta y} = \frac{\Delta y}{\Delta}$$

$$\Psi_F(x) = \Psi_{F0} + \Delta\Psi_F$$

$$\frac{\partial \Psi_F}{\partial \Delta \Psi_F} = 1$$

$$F_h(x) = \sqrt{F_{xh}^2 + F_{yh}^2}$$

$$\frac{\partial F_h}{\partial F_{xh}} = \frac{F_{xh}}{F_h} \quad \frac{\partial F_h}{\partial F_{yh}} = \frac{F_{yh}}{F_h}$$

$$\psi_t(x) = \tan^{-1}\left(\frac{F_{yt}}{F_{xt}}\right)$$

$$\frac{\partial \psi_t}{\partial F_{xt}} = -\frac{F_{yt}}{F_t^2} \quad \frac{\partial \psi_t}{\partial F_{yt}} = \frac{F_{xt}}{F_t^2}$$

$$\psi_{hT}(x) = \tan^{-1}\left(\frac{F_{yh}}{F_{xh}}\right)$$

$$\frac{\partial \psi_{hT}}{\partial F_{xh}} = -\frac{F_{yh}}{F_h^2} \quad \frac{\partial \psi_{hT}}{\partial F_{yh}} = \frac{F_{xh}}{F_h^2}$$

$$\begin{bmatrix} F_{xm}(x) \\ F_{ym}(x) \\ N_{zm}(x) \end{bmatrix} = \mathbf{K}_F \begin{bmatrix} \Delta x \\ \Delta y \\ \Delta\Psi_F \end{bmatrix}$$

$$\begin{bmatrix} \partial F_{xm}/\partial \Delta x & \partial F_{xm}/\partial \Delta y & \partial F_{xm}/\partial \Delta\Psi_F \\ \partial F_{ym}/\partial \Delta x & \partial F_{ym}/\partial \Delta y & \partial F_{ym}/\partial \Delta\Psi_F \\ \partial N_{zm}/\partial \Delta x & \partial N_{zm}/\partial \Delta y & \partial N_{zm}/\partial \Delta\Psi_F \end{bmatrix} = \mathbf{K}_F$$

A.2.3 Environmental Load Functions. Suppose the relative heading between a vessel and a particular environmental load is θ, where $\theta(x) = \Theta - \Psi(x)$, Θ is the absolute heading of the environmental load, $\Psi(x)$ is the heading of the vessel, and $\theta_i \leqslant \theta(x) \leqslant \theta_{i+1}$.

Then, $F(\theta(x)) = \alpha(\theta(x) - \theta_i)^3 + \beta(\theta(x) - \theta_i)^2 + \gamma(\theta(x) - \theta_i) + \delta\alpha$, where β, γ, and δ are polynomial interpolating coefficients.

The coefficients are chosen so that the polynomial interpolates the environmental load function exactly at θ_i and θ_{i+1}. If higher order polynomials are used, the remaining coefficients are chosen to provide continuity of the derivatives of the interpolating polynomial. In general, the nonzero partial derivatives of the environmental loads are of the form

$$\frac{\partial F}{\partial \Psi} = \frac{dF}{d\theta}\frac{\partial \theta}{\partial \Psi}$$

where

$$\frac{dF}{d\theta} = 3\alpha(\theta(x) - \theta_i)^2 + 2\beta(\theta(x) - \theta_i) + \gamma$$

$$\frac{\partial \theta}{\partial \Psi} = -1$$

The gradient of the net environmental load is the sum of the gradients of loads from wind, current, swell, and local waves. Other complex gradients can be derived from those given above.

A.2.4 Miscellaneous Constraint Functions

$$\psi_T(x) = \Psi_T - \Psi_F(x) - 180$$

$$\nabla\psi_T = \nabla\Psi_T - \nabla\Psi_F$$

$$\psi_{hF}(x) = \Psi_T - 180 - \Psi_F(x) + \psi_{hT}(x)$$

$$\nabla\psi_{hF} = \nabla\Psi_T - \nabla\Psi_F + \nabla\psi_{hT}$$

A.2.5 Equilibrium Constraints

$$c(x) = \begin{bmatrix} F_{xeT}(x) + F_{xt} + F_{xh} \\ F_{yeT}(x) + F_{yt} + F_{yh} \\ N_{zeT}(x) - \frac{1}{2} l_{bpT} F_{yt} + \frac{1}{2} l_{bpT} F_{yh} \\ F_{xeF}(x) + F_h(x)\cos(\psi_{hF}(x)) - F_{xm}(x) \\ F_{yeF}(x) + F_h(x)\sin(\psi_{hF}(x)) - F_{ym}(x) \\ N_{zeF}(x) + \frac{1}{2} l_{bpF} F_h(x)\sin(\psi_{hF}(x)) - N_{zm}(x) \end{bmatrix}$$

$$\nabla c_1 = \nabla F_{xeT} + \nabla F_{xt} + \nabla F_{xh}$$

$$\nabla c_2 = \nabla F_{yeT} + \nabla F_{yt} + \nabla F_{yh}$$

$$\nabla c_3 = \nabla N_{zeT} - \frac{1}{2} l_{bpT} \nabla F_{yt} + \frac{1}{2} l_{bpT} \nabla F_{yh}$$

$$\nabla c_4 = \nabla F_{xeF} - F_h \sin \psi_{hF} \nabla \psi_{hF} + \cos \psi_{hF} \nabla F_h - \nabla F_{xm}$$

$$\nabla c_5 = \nabla F_{yeF} + F_h \cos \psi_{hF} \nabla \psi_{hF} + \sin \psi_{hF} \nabla F_h - \nabla F_{ym}$$

$$\nabla c_6 = \nabla N_{zeF} + \frac{1}{2} l_{bpF} (F_h \cos \psi_{hF} \nabla \psi_{hF} + \sin \psi_{hF} \nabla F_h) - \nabla N_{zm}$$

References

[1] Henriques, C. C. D., 2000, "Petrobras Experience on the Mooring of Conventional Shuttle Tankers to Dynamically Positioned FPSOs," in *Proceedings of the International Offshore and Polar Engineering Conference*, Number 1, pp. 323–330.

[2] Morandini, C., Legerstee, F., Francois, M., and Raposo, C. V., 2001, "Numerical Analysis of FPSO Offloading Operations," in *Proceedings of the International Conference on Offshore Mechanics and Arctic Engineering*, Number 1, pp. 11–20.

[3] Morandini, C., Legerstee, F., and Mombaerts, J., 2002, "Criteria for Analysis of Offloading Operation," in *Proceedings of the Annual Offshore Technology Conference*, pp. 2751–2755.

[4] Lee, D. H., and Choi, H. S., 2000, "Dynamic Analysis of FPSO-Shuttle Tanker System," in *Proceedings of the International Offshore and Polar Engineering Conference*, Number 1, pp. 302–307.

[5] Morishita, H. M., and De Souza, J. R., Jr., 2002, "Dynamic Behavior of a DICAS FPSO and Shuttle Vessel Under the Action of Wind, Current and Waves," in *Proceedings of the International Offshore and Polar Engineering Conference*, Number 12, pp. 142–150.

[6] Booker, A. J., Dennis, J. E., Jr., Frank, P. D., Serafini, D. B., Torczon, V., and Trosset, M. W., 1999, "A Rigorous Framework for Optimization of Expensive Functions by Surrogates," Marine Mammal Sci., **17**(1), pp. 1–13.

[7] Jain, R. K., 1980, "A Simple Method of Calculating the Equivalent Stiffness in Mooring Cables," Appl. Ocean. Res., **2**(3), pp. 139–142.

[8] Inoue, Y., and Islam, M. R., 1999, "Comparative Study of Numerical Simulation and the Experimental Results for a Parallely Connected FPSO and LNG in Waves," in *Proceedings of the International Offshore and Polar Engineering Conference*, Number 1, pp. 360–367.

[9] Guedes, S. C., Fonseca, N., and Pascoal, R., 2001, "Experimental and Numerical Study of the Motions of a Turret Moored FPSO in Waves," in *Proceedings of the International Conference on Offshore Mechanics and Arctic Engineering*, Number 1, pp. 185–193.

[10] 1994, Prediction of Wind and Current Loads on VLCCs, Oil Companies International Marine Forum (OCIMF), 2nd ed.

[11] Codiglia, R., Contento, G., D'Este, F., Galeazzi, F., Sole, V., Coan, A., and Spezzati, M., 2002, "Experimental Study on a Spread Catenary Mooring for FPSO," in *Proceedings of the International Offshore and Polar Engineering Conference*, Number 12, pp. 132–141.

[12] Wilkerson, S. M., 2005, "An Optimization Algorithm for Minimum Weight Design of Steel Frames With Nonsmooth Stress Constraints," Ph.D. thesis, Rice University, Houston, TX.

[13] Eldred, M. S., and Dunlavy, D. M., 2006, "Formulations for Surrogate-Based Optimization With Data Fit, Multifidelity, and Reduced-Order Models," in *Proceedings of the 11th AIAA/ISSMO Multidisciplinary Analysis and Optimization Conference*, Portsmouth, VA, pp. 1–20.